Macromolecules
ARTICLE

Macromolecules **2010**, *43*, 2413–2420 **2413**
DOI: 10.1021/ma902508n

Layer-by-Layer Codeposition of Polyelectrolyte Complexes and Free Polyelectrolytes for the Fabrication of Polymeric Coatings

Ling Zhang and Junqi Sun*

State Key Laboratory of Supramolecular Structure and Materials, College of Chemistry, Jilin University, Changchun 130012, People's Republic of China

Received November 12, 2009; Revised Manuscript Received February 1, 2010

ABSTRACT: The layer-by-layer (LbL) codeposition of polyelectrolyte−polyelectrolyte complexes (PECs) and free polyelectrolytes with oppositely charged polyelectrolytes for the fabrication of polymeric films has been systematically investigated. Aqueous dispersions containing positively charged diazoresin (DAR)−poly(acrylic acid) (PAA) complexes (denoted as DAR-PAA) and free DAR were used as the dipping solutions for LbL film fabrication with PAA. Simultaneous deposition of DAR-PAA complexes and free DAR with PAA took place under a nondrying LbL deposition process that produced bilayered thick polymeric films with the hierarchical PAA/DAR-PAA coatings rooting in the underlying continuous PAA/DAR films. The structure of the bilayered polymeric films depends largely on the ratio of DAR-PAA complexes to free DAR in the dipping solution. The more rapid deposition of PAA/DAR-PAA coatings than that of the PAA/DAR films accounts for the formation of bilayered polymeric films because DAR-PAA complexes have larger dimensions than DAR in solution. The bilayered polymeric coatings with hierarchical structures rooting in continuous films have enhanced adhesion with the underlying substrates because of the increased contacting area. After chemical vapor deposition of a layer of fluoroalkylsilane, the bilayered polymeric coatings can be easily converted into superhydrophobic. In contrast, the LbL codeposition of DAR-PAA complexes and DAR with PAA produces thin and compact films without bilayered structures when a N_2 drying step is conducted after each layer deposition. The present study is meaningful in deeply understanding the deposition behavior and structure tailor of LbL assembled films using PECs as building blocks.

Introduction

The layer-by-layer (LbL) assembly technique, which was developed by Decher and coworkers in the early 1990s, has been demonstrated to be a convenient and versatile method to fabricate film materials with precise control of the chemical composition and architecture on micro- and nanoscales.[1,2] The LbL assembly technique is particularly suitable for film deposition on nonflat surfaces with large areas.[3] Up to now, various kinds of materials, including almost all kinds of polyions, inorganic materials,[4] dendrimers,[5] oligo-charged organic molecules,[6] micelles,[7] and biomacromolecules[8] have been successfully incorporated into LbL assembled films. These films can find multiple applications in areas such as antireflection coatings,[4b,7c,9] superhydrophobic surfaces,[10] nonlinear optics,[11] biosensors,[12] cell adhesion or resistance coatings,[2b,13] drug delivery systems,[3e,14] proton exchange membrane,[15] solar-energy conversion,[16] separation membranes,[17] and so forth. The search for new building blocks is a prerequisite for the fabrication of LbL assembled advanced functional film materials, which is of the same importance as the exploration of driving force for LbL assembly technique. In general, polymeric building blocks possessing versatile structures in solution are helpful to obtain polymeric films with well-tailored structures as well as functionalities. For instance, LbL assembled polymeric films composed of weak polyelectrolytes have more diverse and easily tailored film structures than those of strong polyelectrolytes because the configurations of weak polyelectrolytes are more easily tailored in solution and films than strong ones.[9a,18] Therefore, materials with diverse and highly controllable structures in solution are always favored for the fabrication of LbL assembled functional film materials.

Polyelectrolyte−polyelectrolyte complexes (PECs), formed mainly by electrostatic interactions between oppositely charged macromolecules, represent a special class of polymeric compounds possessing versatile and easily tailored compositions and structures in solution.[19] Compared with simplex linear polymers, PECs have an abundance of compositions, relatively large dimensions, and diverse structures, which can all be easily tailored by changing the parameters such as mixing ratio, concentration, solution pH, ionic strength, temperature, and so on during or after the formation of PECs.[19] In the past several decades, much effort has been expended to use PECs in various fields, such as nanocarriers for the delivery of drugs, water purification, cosmetics, and so forth.[20] Nonstoichiometric PECs, which can be either positively or negatively charged depending on the excessive component, can be used as building blocks for LbL assembled film fabrication.[21] In our previous study, we proved that the use of PECs as building blocks for LbL film fabrication has at least two advantages: (i) PECs provide a facile way to well tailor the structures as well as the functionalities of the LbL assembled films because of the easily tailored structures of PECs in solution or even in films through post film treatments.[22] (ii) The large dimensions of PECs enable the rapid fabrication of LbL assembled functional films, especially for those with micrometer thickness.[7e,23]

Although PECs are practically useful for the fabrication of LbL assembled functional film materials, the precise understanding of the deposition behavior and structural tailoring of LbL assembled films using PECs as building blocks remains challenging because of the complexity of PECs in solutions. For instance,

*Corresponding author. Fax: 0086-431-85193421. E-mail: sun_junqi@jlu.edu.cn.

Published on Web 02/09/2010

Scheme 1. (a) Chemical Structure of DAR and (b) Photoreaction of DAR and PAA

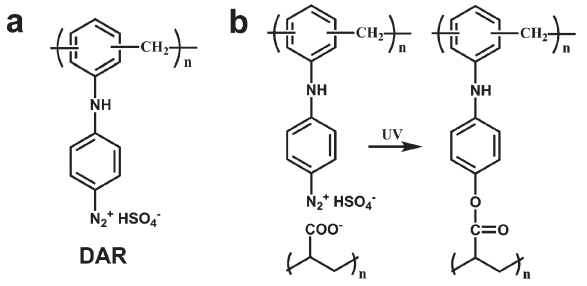

free polyelectrolytes usually exist in the dispersions of PECs because there is a balance between the PECs and free polyelectrolytes, especially for those with one kind of polyelectrolyte being in excess.[19a,24] The separation of the free polyelectrolytes may break the balance and induce the partial dissociation of the PECs.[24] In this case, the particles of the PECs and free polyelectrolytes are involved simultaneously in the LbL deposition with partner species to produce multilayer films. The elucidation of the simultaneous LbL deposition behaviors of PECs and the coexisted free polyelectrolytes is not only academically important but also helpful for designing functional film materials. The present work aims to understand the deposition behavior and structural tailoring of the LbL assembled films when PECs and free polyelectrolytes coexist in the dipping solutions. To do so, positively charged PECs of diazoresin (DAR) and poly(acrylic acid) (PAA) (denoted as DAR-PAA) with a molar excess of DAR were prepared and alternately deposited with PAA to fabricate LbL assembled polymeric films. Simultaneous LbL deposition of positively charged DAR-PAA complexes and free DAR with negatively charged PAA were observed with systematically changing the amount of free DAR in the dipping solution. As a result, polymeric coatings with the hierarchical structures of PAA/DAR-PAA rooting in the underlying continuous PAA/DAR films were produced. These kinds of films, with the hierarchical structures on the top and continuous film on the bottom, are believed to have strong adhesion with the underlying substrate and can be used as superhydrophobic coatings after chemical vapor deposition of a layer of fluoroalkylsilane.

Experimental Section

Materials. Poly(diallyldimethylammonium chloride) (PDDA, M_w ca. 100 000−200 000), poly(acrylic acid) (PAA, M_w ca. 1800 and 100 000) were purchased from Sigma-Aldrich. 1*H*,1*H*,2*H*, 2*H*-perfluorooctyltriethoxysilane (POTS) was purchased from Degussa. All chemicals were used without further purification. DAR was synthesized according to the literature procedure.[25] The chemical structure of DAR is shown in Scheme 1a. The molecular weight (M_n) of DAR was ~2500. Deionized water was used for all of the LbL film fabrication.

Preparation of DAR-PAA Dispersions. Positively charged DAR-PAA dispersions were prepared by dropwise adding 1 mg/mL PAA (M_w ca. 1800) solution in 1 mg/mL DAR solution under intense stirring. The DAR-PAA dispersions with different mixing ratio were prepared with the feed monomer molar ratio of DAR to PAA being 1:0.4, 1:0.2, and 1:0.1, respectively. For simplicity, they were denoted as DAR-$PAA_{0.4}$, DAR-$PAA_{0.2}$, and DAR-$PAA_{0.1}$ dispersions, respectively.

To evaluate the amount of free DAR in aqueous DAR-PAA dispersions, we dialyzed the as-prepared DAR-PAA dispersions by using dialysis membrane with a MWCO of 3500 in pH 3.0 water, which had the same pH as that of the DAR-PAA dispersions. The dialysate was collected to determine the amount of uncomplexed DAR in the original DAR-PAA dispersions. The DAR-PAA complexes after dialysis were denoted as DAR-PAA_d for short. It is worth noting that the dialysis was carried out in the dark to prevent the photolysis of DAR.

Coating Preparation. A substrate of silicon wafer or quartz was immersed in a slightly boiled piranha solution (1:3 mixture of 30% H_2O_2 and 98% H_2SO_4) for 20 min. *Caution: Piranha solution reacts violently with organic materials and should be handled carefully*. After being rinsed with ample water and dried with N_2 flow, the resulting substrate was immersed in aqueous cationic solution of 1 mg/mL PDDA for 20 min to obtain a positively charged surface. The LbL assembled films using aqueous DAR-PAA dispersions as the dipping solutions are denoted as [PAA/(DAR-PAA+DAR)]*n (n refers to the number of deposition cycles) films because the aqueous dispersions contain both DAR-PAA complexes and free DAR. The LbL deposition of PAA/(DAR-PAA+DAR) films was conducted in the dark automatically by a programmable dipping machine. The PDDA-modified silicon wafer or quartz was first immersed in an aqueous PAA solution (pH 3.5, 1 mg/mL, M_w ca. 100 000) for 15 min, followed by rinsing with water three times for 1 min each time. Then, the substrate was immersed in aqueous DAR-PAA dispersion (pH 3.0) for another 15 min and rinsed in three water baths for 1 min each time. No drying step was used in the deposition procedure unless it was in the last layer. Multilayer films of [PAA/(DAR-PAA+DAR)]*n can be fabricated by repeating these steps in a cyclic fashion. In a control experiment, LbL assembled PAA/(DAR-PAA+DAR) films with drying steps after each layer deposition were fabricated in a similar way as those of PAA/(DAR-PAA+DAR) films, except that a drying step using N_2 flow was performed after the substrate was washed in water.

Photo-cross-linking of the LbL assembled PAA/(DAR-PAA+DAR) films was conducted by irradiating the films with a 250 W UV lamp at a distance of 5 cm from the source for 20 min (5 min for each time to prevent the films from high temperature) to ensure that the reaction proceeded completely. Under UV irradiation, diazonium groups of DAR in LbL assembled PAA/(DAR-PAA+DAR) films decompose to produce cationic phenyl groups that react with nucleophile groups of carboxylate in PAA to form carboxylate esters (Scheme 1b).[26] Therefore, covalently cross-linked PAA/(DAR-PAA+DAR) films were obtained after UV irradiation.

Chemical Vapor Deposition of POTS. The substrate deposited with PAA/(DAR-PAA+DAR) coatings was placed in a sealed vessel, and a few drops of POTS were dispensed on the bottom of the vessel. There was no direct contact between the substrate and the drops. The vessel was put in an oven at 120 °C for 2 h to enable the vapor of POTS to react with the −OH groups on the substrate surface. Finally, the substrate was taken out of the vessel and placed in an oven at 150 °C for another 2 h to volatilize the unreacted POTS molecules on the substrate.

Characterization. Dynamic light scattering (DLS) studies and ζ-potential measurements were carried out on a Malvern Nano-ZS zetasizer at room temperature. The measurements were made at a scattering angle of $\theta = 173°$ at 25 °C using a He−Ne laser with a wavelength of 633 nm. UV−vis absorption spectra were recorded with a Shimadzu UV-2550 spectrophotometer. Multilayer film fabrication was conducted by Dipping Robot DR-3, Riegler & Kirstein GmbH at room temperature. Scanning electron microscopy (SEM) images were obtained on a XL30 ESEM FEG scanning electron microscope. The height of the hierarchical structures derive from the LbL deposition of DAR-PAA complexes with PAA was calculated from the surface of the substrate and was the average value obtained from three separate cross-sectional SEM images. For each SEM image, 40 equidistant positions were measured. Therefore, the height of the hierarchical structures was the average value of 120 positions. A dektak 150 surface profiler using a 5 μm stylus tip with 3 mg stylus force was used to characterize the topography and the root-mean-square (rms) roughness of the LbL assembled coatings (500 × 500 μm^2). The static contact angles

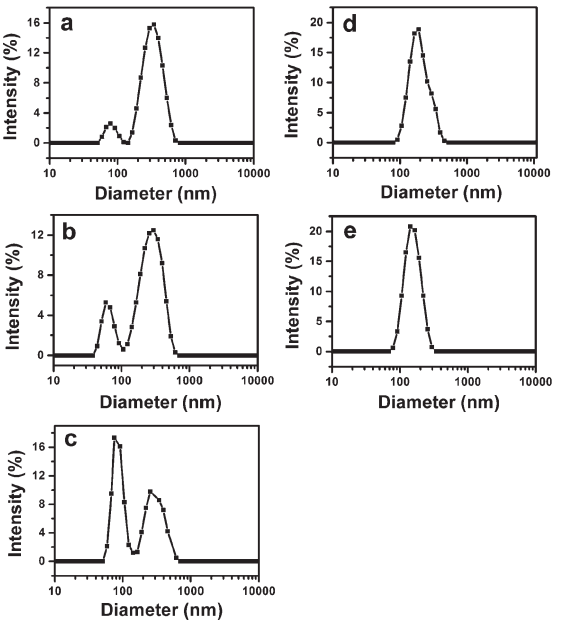

Figure 1. Hydrodynamic diameter distribution curves of DAR-PAA dispersions with mixing ratio of DAR to PAA being (a) 1:0.4, (b) 1:0.2, and (c) 1:0.1, respectively. Hydrodynamic diameter distribution curves of (d) DAR-$PAA_{d0.4}$ and (e) DAR-$PAA_{d0.2}$ complexes.

and sliding angles were measured with a commercial contact angle system (DataPhysics, OCA 20) at ambient temperature using a 4 μL water droplet as the indicator.

Results and Discussion

Preparation of DAR-PAA Dispersions. Excessive polycation DAR was used to complex with polyanion PAA by electrostatic interaction as a main driving force. The pH of the aqueous DAR-PAA dispersions was adjusted to 3.0, at which the aqueous DAR-PAA dispersions were stable and homogeneous. Increasing the pH of the aqueous DAR-PAA dispersions to 4.0 would cause the precipitation of the DAR-$PAA_{0.4}$ complexes because PAA contains more carboxylate groups and has a stronger interaction with positively charged DAR. When the pH of the aqueous DAR-PAA dispersion is decreased to 2.0, stable DAR-PAA complexes cannot form because PAA contains a few carboxylate groups at such a low pH. Therefore, aqueous DAR-PAA dispersions with a pH of 3.0 were prepared for LbL film fabrication. Electrophoresis measurements show that the DAR-$PAA_{0.4}$, DAR-$PAA_{0.2}$, and DAR-$PAA_{0.1}$ dispersions at pH 3.0 are positively charged with their corresponding ζ potentials being +22.6, +26.4, and +37.5 mV, respectively, which further demonstrates that DAR is molar excessive in the DAR-PAA dispersions. DLS measurements were used to characterize the size distribution of the DAR-PAA dispersions. As shown in Figure 1a, the DLS curve of DAR-$PAA_{0.4}$ dispersion exhibits bimodal size distributions with the hydrodynamic diameter of the smaller particles center at 78.8 nm and the larger ones with a broad distribution having a maximum at 342.0 nm. Similarly to DAR-$PAA_{0.4}$ dispersion, two size fractions have also been observed for the freshly prepared DAR-$PAA_{0.2}$ and DAR-$PAA_{0.1}$ dispersions, with the smaller particles maximized at 68.1 and 75.2 nm and the larger ones at 295.3 and 255.0 nm, respectively (Figure 1b,c). Dialysis was conducted to separate free DAR from the DAR-PAA dispersions. After 2 min of dialysis, characteristic UV−vis absorbance of DAR could be observed for the dialysates of the DAR-PAA dispersions with mixing ratio of 0.4, 0.2, and 0.1, which confirms the existence of free DAR in the DAR-PAA dispersions. Therefore, the as-prepared DAR-PAA dispersions can be considered to be a complicated system consisting of excessive free DAR, small primary complex particles, and large complex particles of DAR-PAA.

After dialysis for 1 week in the dark, the dialysates were collected, and the amount of excessive DAR in the as-prepared DAR-PAA dispersions was calculated because the absorbance of DAR in aqueous solution obeys the Lambert−Beer law. After dialysis, about 46, 66, and 78% of the whole DAR were removed from the as-prepared DAR-PAA dispersions with a mixing molar ratio of DAR to PAA being 1:0.4, 1:0.2, and 1:0.1, respectively. The dialyzed DAR-PAA complexes are still nonstoichiometric and have an excess of DAR, with the ζ potentials of DAR-$PAA_{d0.4}$ and DAR-$PAA_{d0.2}$ being +10.3 and +12.0 mV, respectively. The excessive DAR can prevent the accumulation or precipitation of the DAR-PAA complexes in aqueous dispersions. DLS measurements show that after dialysis, a single well-resolved peak around 190.1 and 141.8 nm is observable for DAR-$PAA_{d0.4}$ and DAR-$PAA_{d0.2}$, respectively (Figure 1d,e). The dialyzed DAR-PAA complexes became smaller and more uniform in size than their corresponding complexes before dialysis. With the gradual removal of free DAR, the balance between free DAR and DAR-PAA complexes in their aqueous dispersions is broken, which leads to the dissociation of the original DAR-PAA complexes. The DAR-PAA complexes with smaller sizes are easier to dissociate than larger ones because of their higher surface-to-volume ratio. The absence of the DLS peak around 70 nm indicates the complete dissociation of the small DAR-PAA complexes. Meanwhile, the dissociation of the large DAR-PAA complexes leads to the decrease in their particle size. DLS measurements show that no particles can be detected in the DAR-$PAA_{0.1}$ dispersion after dialysis.

LbL Fabrication of PAA/(DAR-PAA+DAR) Coatings. Aqueous DAR-PAA dispersions comprising free DAR and nonstoichiometric DAR-PAA complexes can be used as dipping solutions for LbL film fabrication with polyanion PAA based on electrostatic interaction as the main driving force. No drying step was used during the film deposition procedure until it was in the last layer. All films were characterized after they were cross-linked under UV irradiation. SEM was used to characterize the surface morphologies of the PAA/(DAR-$PAA_{0.2}$+DAR) films with different deposition cycles. The surface of the UV-irradiated [PAA/(DAR-$PAA_{0.2}$+DAR)]*15 film is mainly scattered with separated and aggregated particles (Figure 2a,b). As confirmed later, these particles are DAR-PAA complexes and aggregates of DAR-PAA complexes glued by PAA. With increasing number of film deposition cycles, the amount of the deposited particles increase, and these particles associate more intimately to form larger aggregates (Figure 2c−f). Take the [PAA/(DAR-$PAA_{0.2}$+DAR)]*50 film, for instance, hierarchical structures with lateral dimensions of several micrometers are observed (Figure 2e,f). The enlarged SEM image in Figure 2f clearly discloses that the hierarchical structures are composed of multistep-aggregated particles of DAR-PAA complexes glued by PAA. The 3D topographies of the PAA/(DAR-$PAA_{0.2}$+DAR) films with different deposition cycles were further investigated by surface profiler because the size and height of the microstructures on the films were too large to measure by AFM. 3D profilometry measurements demonstrate that islandlike structures appear on the surface of the LbL deposited PAA/(DAR-$PAA_{0.2}$+DAR) films. The density and dimension of islands increase

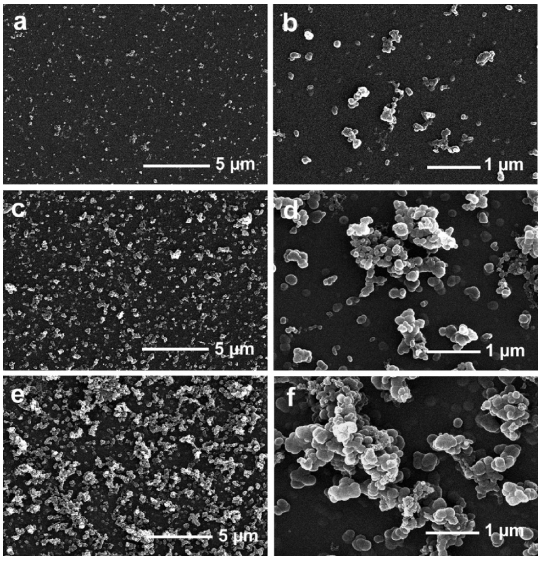

Figure 2. Top-view SEM images of the UV-irradiated PAA/(DAR-$PAA_{0.2}$+DAR) coatings with deposition cycles of (a,b) 15, (c,d) 30, and (e,f) 50.

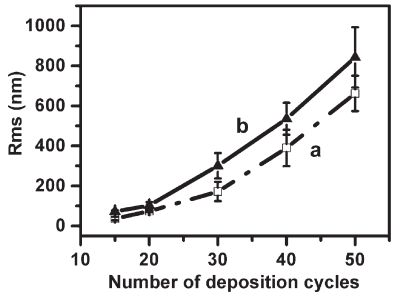

Figure 3. Dependence of rms roughness of the PAA/(DAR-$PAA_{0.2}$+DAR) (curve a) and PAA/(DAR-$PAA_{0.4}$+DAR) (curve b) coatings as a function of the number of coating deposition cycles. Films with a scanning area of 500 × 500 μm^2 were measured.

with increasing number of film deposition cycles. Figure 3 indicates that the root-mean-square (rms) roughness of the PAA/(DAR-$PAA_{0.2}$+DAR) films increases with increasing number of film deposition cycles.

The structures of the PAA/(DAR-$PAA_{0.2}$+DAR) films with different deposition cycles are further disclosed by their cross-sectional SEM images. As shown in Figure 4, all PAA/(DAR-$PAA_{0.2}$+DAR) coatings are recognized by their bilayer structures, which comprise the underlying continuous layer that is flat and uniform and the top discontinuous layer, which has hierarchical structures. As summarized in Figure 4e, the thickness of the continuous films and the height of the hierarchical structures increase almost linearly with increasing number of film deposition cycles, with an increment of 1.9 ± 0.3 and 14.0 ± 2.4 nm per deposition cycle for the continuous film and the hierarchical structures, respectively. This result confirms the simultaneous deposition of the continuous films and the hierarchical structures. We conclude that the continuous films originate from the LbL deposition of PAA with free DAR in the aqueous DAR-$PAA_{0.2}$ dispersion, whereas the hierarchical structures correspond to the alternate deposition of PAA with the positively charged DAR-PAA complexes. The LbL deposition of DAR-PAA complexes with PAA leads to a discontinuous and thick coating with hierarchical structures because of the loosely stacked sphere-like DAR-PAA complexes. The deposition of PAA/DAR films takes place

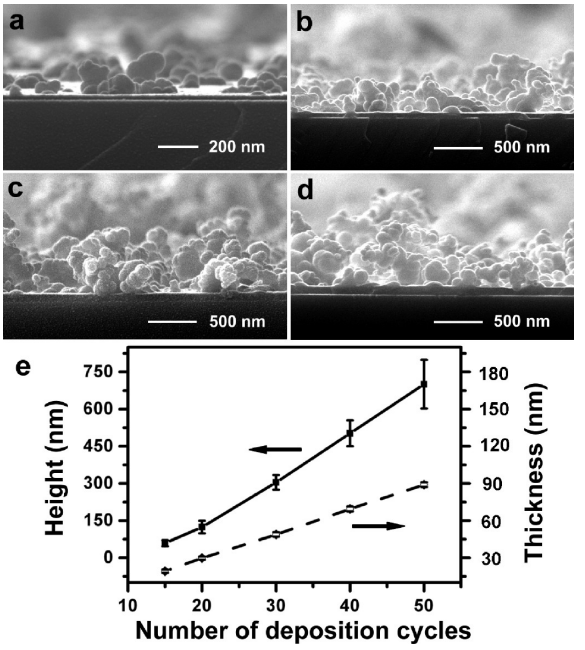

Figure 4. Cross-sectional SEM images of UV-irradiated PAA/(DAR-$PAA_{0.2}$+DAR) coatings with deposition cycles being (a) 15, (b) 30, (c) 40, and (d) 50, respectively. (e) Dependence of the height of the hierarchical structures (■) and the thickness of the continuous films (○) as a function of the number of coating deposition cycles.

simultaneously with the deposition of PAA/DAR-PAA discontinuous films but proceeds more slowly than that of PAA/PAA-DAR because of the smaller dimensions of free DAR than DAR-PAA complexes. Therefore, PAA/DAR films occupy the interstices of PAA/DAR-PAA coatings. As a result, polymeric coatings with the hierarchical structures of PAA/DAR-PAA rooting in the underlying PAA/DAR films were finally obtained. The thickness increment of 1.9 ± 0.3 nm per deposition cycle for the continuous PAA/DAR film is consistent with the thickness of one bilayer of PAA/DAR reported in our previous publication,[26] endorsing further that the LbL assembled PAA/DAR films correspond to the underlying films in the bilayered PAA/(DAR-$PAA_{0.2}$+DAR) films. The height of one cycle of the PAA/DAR-PAA film is smaller when compared with the hydrodynamic diameters of DAR-PAA complexes in solution because deformation and shrinkage of the complexes usually occur when deposited on a solid surface.[23] Meanwhile, the low surface coverage of the DAR-PAA complexes, as disclosed in Figure 2, also suppresses the thickness increase in the PAA/DAR-PAA films.

Dependence of Film Structures on Mixing Ratio of DAR-PAA Dispersions. We further investigated the simultaneous LbL deposition of positively charged DAR-PAA complexes and DAR with negatively charged PAA by systematically changing the amount of free DAR in the aqueous DAR-PAA dispersions. The cross-sectional SEM image shown in Figure 5a indicates that the [PAA/(DAR-$PAA_{0.4}$+DAR)]*50 film has a similar bilayer structure as that of [PAA/(DAR-$PAA_{0.2}$+DAR)]*50 film, where the hierarchical structures of PAA/DAR-PAA root in the continuous PAA/DAR coating. As shown in Figure 5b, the aggregated structures in the [PAA/(DAR-$PAA_{0.4}$+DAR)]*50 film have larger dimensions and higher density than those in [PAA/(DAR-$PAA_{0.2}$+DAR)]*50 film. The thickness of the underlying PAA/DAR and height of the PAA/DAR-$PAA_{0.4}$ hierarchical structures in PAA/(DAR-$PAA_{0.4}$+DAR) films with different deposition cycles are summarized in Figure 5c.

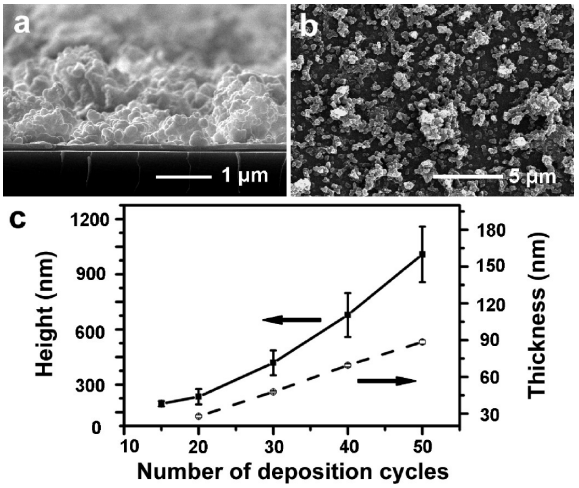

Figure 5. (a) Cross-sectional and (b) top-view SEM images of UV-irradiated [PAA/(DAR-PAA$_{0.4}$+DAR)] *50 coatings. (c) Dependence of the height of the hierarchical structures (■) and the thickness of the continuous films (○) of the PAA/(DAR-PAA$_{0.4}$+DAR) films as a function of the number of coating deposition cycles.

A linear increase of 1.6 ± 0.4 nm per deposition cycle is obtained for the underlying PAA/DAR films. This value is smaller than that of the PAA/DAR films fabricated using DAR-PAA$_{0.2}$ dispersion because of the lower concentration of free DAR in DAR-PAA$_{0.4}$ dispersion than in DAR-PAA$_{0.2}$ dispersion. With increasing number of film deposition cycles, the height of the PAA/DAR-PAA$_{0.4}$ in PAA/(DAR-PAA$_{0.4}$+DAR) films increases more rapidly than that of PAA/DAR-PAA$_{0.2}$ in PAA/(DAR-PAA$_{0.2}$+DAR) films because of the larger dimensions of DAR-PAA$_{0.4}$ complexes than DAR-PAA$_{0.2}$ complexes in their corresponding aqueous dispersions. For instance, the height of the hierarchical structures in [PAA/(DAR-PAA$_{0.4}$+DAR)]*50 and [PAA/(DAR-PAA$_{0.2}$+DAR)]*50 films are 1144.5 ± 201.2 and 700.4 ± 98.2 nm, respectively. Three-dimensional profilometry measurements in curve b of Figure 3 indicate that the rms roughness of the PAA/(DAR-PAA$_{0.4}$+DAR) films increases more rapidly than those of PAA/(DAR-PAA$_{0.2}$+DAR) films, which is consistent with the larger dimensions of DAR-PAA$_{0.4}$ complexes than those of DAR-PAA$_{0.2}$ complexes in their corresponding dispersions.

The aqueous DAR-PAA$_{0.1}$ dispersion has the highest ratio of free DAR to DAR-PAA complexes. LbL assembled PAA/(DAR-PAA$_{0.1}$+DAR) films fabricated using aqueous DAR-PAA$_{0.1}$ dispersion have the highest thickness for the underlying PAA/DAR and the lowest height for PAA/DAR-PAA$_{0.1}$ when compared with the coatings fabricated using aqueous DAR-PAA$_{0.2}$ and DAR-PAA$_{0.4}$ dispersions. The highest concentration of free DAR and the smallest hydrodynamic diameter of DAR-PAA$_{0.1}$ complexes account for this result. The cross-sectional SEM image of the PAA/(DAR-PAA$_{0.1}$+DAR)*50 film in Figure 6a shows that the underlying (PAA/DAR)*50 film has a thickness of 113.4 ± 1.5 nm, whereas the structures of (PAA/DAR-PAA$_{0.1}$)*50 only protrude out of the underlying (PAA/DAR)*50 film. The aggregations, which are DAR-PAA$_{0.1}$ complexes glued by PAA, have small sizes and low density (Figure 6b). The structures of LbL deposited PAA/(DAR-PAA+DAR) films can be systematically tailored by changing the mixing ratio of aqueous DAR-PAA dispersions. Meanwhile, the dependence of film structure on ratios of free DAR to DAR-PAA complexes supports the fact that simultaneous deposition of free DAR and DAR-PAA complexes with PAA produces the unique coatings with hierarchical structures of PAA/DAR-PAA rooting in continuous PAA/DAR films.

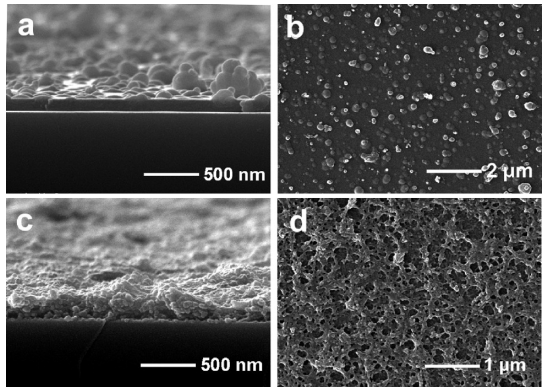

Figure 6. Cross-sectional and top-view SEM images of UV-irradiated (a,b) [PAA/(DAR-PAA$_{0.1}$+DAR)] *50 and (c,d) (PAA/DAR-PAA$_{d0.4}$)*70 coatings.

Dialyzed DAR-PAA$_{d0.4}$ complexes were LbL assembled with PAA to verify further that free DAR and DAR-PAA complexes are important for producing bilayered PAA/(DAR-PAA+DAR) films. The cross-sectional and top-view SEM images of a (PAA/DAR-PAA$_{d0.4}$)*70 film are shown in Figure 6c,d. The (PAA/DAR-PAA$_{d0.4}$)*70 film, which has an average thickness of 247.8 ± 65.7 nm, is macroporous without a bilayer film structure. The macroporous (PAA/DAR-PAA$_{d0.4}$)*70 films originate from the loosely deposited sphere-like PAA/DAR-PAA$_{d0.4}$ complexes with PAA. The thickness of the (PAA/DAR-PAA$_{d0.4}$)*70 films is much thinner than that of the [PAA/(DAR-PAA$_{0.4}$+DAR)]*50 films because of the following: (i) The hydrodynamic diameter of ~190 nm for DAR-PAA$_{d0.4}$ complexes is smaller than that of ~342 nm for DAR-PAA$_{0.4}$ complexes. (ii) The ζ potential of the DAR-PAA$_{d0.4}$ complexes is +10.3 mV, which is much lower than that of +22.6 mV for DAR-PAA$_{0.4}$ complexes before dialysis. The low ζ potential reduces the electrostatic interaction between DAR-PAA$_{d0.4}$ complexes and PAA. Therefore, the deposition of DAR-PAA$_{d0.4}$ complexes on PAA layer becomes difficult. The macroporous PAA/DAR-PAA$_{d0.4}$ films fabricated from alternate deposition of PAA with DAR-PAA complexes without free DAR validate our proposed mechanism for the fabrication of PAA/(DAR-PAA+DAR) films with hierarchical structures rooting in continuous films.

Influence of Drying Steps on Film Fabrication. The drying steps used after each layer deposition can produce a dramatic influence on structures of LbL assembled PAA/(DAR-PAA+DAR) films. The cross-sectional and top-view SEM images of [PAA/(DAR-PAA$_{0.2}$+DAR)]*30 and [PAA/(DAR-PAA$_{0.4}$+DAR)]*30 films fabricated with drying steps after each layer deposition are shown in Figure 7. The [PAA/(DAR-PAA$_{0.2}$+DAR)]*30 and [PAA/(DAR-PAA$_{0.4}$+DAR)]*30 films have an average thickness of 66.2 ± 2.3 and 71.0 ± 3.5 nm, respectively, with one cycle of film being 2.2 and 2.4 nm, respectively (Figure 7a,b). The aggregated particles, which are the LbL assembled PAA/DAR-PAA, are observable but have much lower height and are less aggregated (Figure 7c,d) compared with those in their corresponding films fabricated without drying steps. As demonstrated in our previous publications, hydrated water in PECs is very important to keep their spherical structures when PECs are deposited on a solid surface.[23] Once the hydrated water is removed, the PECs would collapse. A N_2 drying step can remove most of the hydrated water from the DAR-PAA complexes. Concomitantly, the N_2 drying step

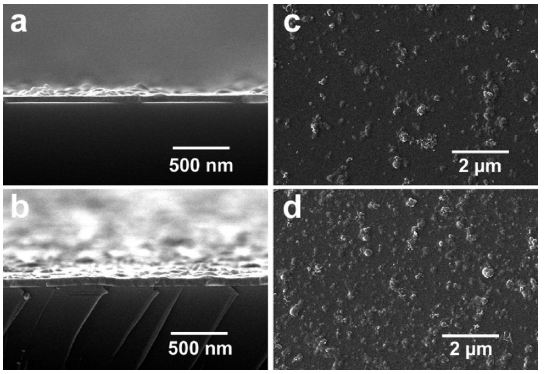

Figure 7. Cross-sectional and top-view SEM images of UV-irradiated (a,c) [PAA/(DAR-PAA$_{0.2}$+DAR)]*30 and (b,d) [PAA/(DAR-PAA$_{0.4}$+DAR)]*30 coatings prepared by a N_2 drying process.

can produce a lateral shear force to spread the DAR-PAA complexes. Consequently, the deposited spherical DAR-PAA complexes collapsed and spread to form a relatively smooth and thin layer after N_2 drying, which slows down the deposition of PAA/DAR-PAA coatings to a speed that is similar to that of PAA/DAR films. Therefore, the LbL codeposition of DAR-PAA complexes and DAR with PAA produces thin and compact films without obvious bilayer structures when a N_2 drying step is used after each layer deposition.

Fabrication of Superhydrophobic Coatings. The LbL codeposition of free DAR and DAR-PAA complexes with PAA produces polymeric coatings with well-tailored PAA/DAR-PAA hierarchical structures rooting in continuous PAA/DAR films. The continuous PAA/DAR films are believed to enhance the adhesion of the whole films with the underlying substrates because of the increased contacting area with the substrates when compared with hierarchical structures deposited directly on solid substrates. Polymeric coatings with well-tailored surface hierarchical structures are widely useful in designing solid surfaces with special wetting properties,[23a,27] structure-related optical devices,[28] and cell or protein adhesion/resistance coatings,[13,29] just to mention a few. We believe that the PAA/(DAR-PAA+DAR) coatings with PAA/DAR-PAA hierarchical structures rooting in continuous PAA/DAR films have multiple applications because their structures can be tailored conveniently. We demonstrated herein that the PAA/(DAR-PAA+DAR) films with hierarchical structures can be readily converted to be superhydrophobic after chemical vapor deposition of a layer of POTS. The wettability of the PAA/(DAR-PAA$_{0.2}$+DAR) and PAA/(DAR-PAA$_{0.4}$+DAR) films with different deposition cycles was characterized by the contact angle instruments using a 4 μL water droplet as the indicator. As shown in Figure 8a, the water contact angle (CA) of the PAA/(DAR-PAA$_{0.2}$+DAR) films increases gradually with increasing number of film deposition cycles. The increased CA is highly related to the gradually increased surface roughness with more layers being deposited. After 30 deposition cycles, the CA of the PAA/(DAR-PAA$_{0.2}$+DAR) film reaches 153.9°. The [PAA/(DAR-PAA$_{0.2}$+DAR)]*30 film exhibits a high superhydrophobic adhesive property toward water. A 4 μL water droplet on the surface of [PAA/(DAR-PAA$_{0.2}$+DAR)]*30 film can maintain the sphere shape when the surface is faced up or even turned upside down (inset in Figure 8a). Superhydrophobic surfaces with high adhesive force to liquids, which mimic the gecko mechanism, show their potential applications in the areas such as liquid transportation with no lost volume, traced analysis, and

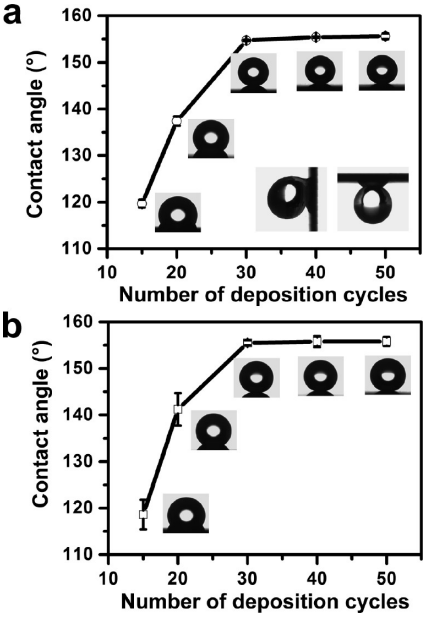

Figure 8. Dependence of contact angles of UV-irradiated (a) PAA/(DAR-PAA$_{0.2}$+DAR) and (b) PAA/(DAR-PAA$_{0.4}$+DAR) coatings as a function of film deposition cycles. Inset in part a shows a 4 μL water droplet on the surface of a [PAA/(DAR-PAA$_{0.2}$+DAR)]*30 coating when the coating is faced down and turned upside.

innovative design of microfluidic devices.[30] When the number of film deposition cycles exceeds 40, the PAA/(DAR-PAA$_{0.2}$+DAR) films become superhydrophobic with low sliding angles. The [PAA/(DAR-PAA$_{0.2}$+DAR)]*40 and [PAA/(DAR-PAA$_{0.2}$+DAR)]*50 films have a CA of 155.4 and 155.6°, respectively. The sliding angle of such coatings is as low as 1°. The CA of PAA/(DAR-PAA$_{0.4}$+DAR) films shows a similar trend as that of PAA/(DAR-PAA$_{0.2}$+DAR) films as the number of film deposition cycles increases (Figure 8b). The PAA/(DAR-PAA$_{0.4}$+DAR) films become superhydrophobic with low sliding angles of 1° when the number of film deposition cycles exceeds 30. The [PAA/(DAR-PAA$_{0.4}$+DAR)]*30 film has a CA of 155.5° and sliding angle of 1°, demonstrating a more rough surface of [PAA/(DAR-PAA$_{0.4}$+DAR)]*30 films than [PAA/(DAR-PAA$_{0.2}$+DAR)]*30 films.

We examined the stability of a superhydrophobic [PAA/(DAR-PAA$_{0.4}$+DAR)]*50 coating by rubbing the coating with a piece of filter paper under different pressures. The superhydrophobic coating was rubbed by dragging the coating along the filter paper to a distance of 5 cm each time. After rubbing for 20 times, its wettability was measured. Under a pressure of 400 Pa, the rubbed [PAA/(DAR-PAA$_{0.4}$+DAR)]*50 coating still keeps its superhydrophobicity with a CA of 152° and a sliding angle $< 5°$. When the pressure applied on the coating reaches 500 Pa, part of the hierarchical structures on the [PAA/(DAR-PAA$_{0.4}$+DAR)]*50 coating can be destroyed, and the coating is superhydrophobic, but the water droplet cannot roll away. Further increasing the rubbing pressure can completely damage the superhydrophobicity of the coating. The rubbing test shows that the superhydrophobic [PAA/(DAR-PAA$_{0.4}$+DAR)]*50 coating has a satisfactory mechanical robustness because of the covalently cross-linked coating structures. The stability of a superhydrophobic [PAA/(DAR-PAA$_{0.4}$+DAR)]*50 coating was also examined by sonicating the coating in water with a power of 0.15 W/cm^2. The superhydrophobic [PAA/(DAR-PAA$_{0.4}$+DAR)]*50 coating shows no decrease in superhydrophobicity after being sonicated in neutralized or

pH 2.0 water for 5 min. This result also verifies that the [PAA/(DAR-PAA$_{0.4}$+DAR)]*50 coating has a strong adhesion with the underlying substrate.

Conclusions

In the present study, the LbL deposition behaviors of PECs and the coexisted free polyelectrolytes for LbL film fabrication have been elucidated. By using aqueous dispersions containing positively charged DAR-PAA complexes and free DAR as dipping solutions, PAA/(DAR-PAA+DAR) films were fabricated by LbL deposition of positively charged DAR-PAA complexes and free DAR with polyanion PAA. Under a nondrying LbL deposition process, the codeposition of DAR-PAA complexes and DAR with PAA produces bilayered thick polymeric films with the PAA/DAR-PAA hierarchical structures rooting in the underlying continuous PAA/DAR films because of the more rapid deposition of PAA/DAR-PAA than DAR/PAA. In contrast, thin and compact films are obtained when a N_2 drying step is conducted after each layer deposition because N_2 drying can slow down the deposition of the PAA/DAR-PAA. Our previous studies verified that the diverse and easily tailored structures of PECs in solution are helpful in fine tailoring the structure of the LbL assembled films comprising alternately deposited PECs. The present study confirms affirmatively that the structural tailoring of the LbL assembled films using PECs as building blocks can benefit from the addition of free polyelectrolytes in the dipping solutions of PECs. The bilayered polymeric films with hierarchical structures rooting in the underlying continuous films are expected to have diverse functionalities because of their unsymmetrical film structure and easily tailored surface morphologies. In particular, when used as superhydrophobic coatings, the increased contacting area provided by the underlying layer can enhance the adhesion of the coatings with the substrates.

Acknowledgment. This work is supported by the National Natural Science Foundation of China (NSFC grant no. 20974037), the National Basic Research Program (2007CB808000), and the Jilin Provincial Science and Technology Bureau of Jilin Province (20070104).

References and Notes

(1) Decher, G. *Science* **1997**, *277*, 1232–1237.
(2) (a) Hammond, P. T. *Adv. Mater.* **2004**, *16*, 1271–1293. (b) Tang, Z. Y.; Wang, Y.; Podsiadlo, P.; Kotov, N. A. *Adv. Mater.* **2006**, *18*, 3203–3224. (c) Quinn, J. F.; Johnston, A. P. R.; Such, G. K.; Zelikin, A. N.; Caruso, F. *Chem. Soc. Rev.* **2007**, *36*, 707–718. (d) Zhang, X.; Chen, H.; Zhang, H. Y. *Chem. Commun.* **2007**, 1395–1405.
(3) (a) Caruso, F.; Caruso, R. A.; Möhwald, H. *Science* **1998**, *282*, 1111–1114. (b) Thierry, B.; Winnik, F. M.; Merhi, Y.; Tabrizian, M. *J. Am. Chem. Soc.* **2003**, *125*, 7494–7495. (c) Ai, S. F.; Lu, G.; He, Q.; Li, J. B. *J. Am. Chem. Soc.* **2003**, *125*, 11140–11141. (d) Jewell, C. M.; Zhang, J.; Fredin, N. J.; Wolff, M. R.; Hacker, T. A.; Lynn, D. M. *Biomacromolecules* **2006**, *7*, 2483–2491. (e) Wang, L.; Chen, D. D.; Sun, J. Q. *Langmuir* **2009**, *25*, 7990–7994.
(4) (a) Lee, D.; Rubner, M. F.; Cohen, R. E. *Nano Lett.* **2006**, *6*, 2305–2312. (b) Podsiadlo, P.; Sui, L.; Elkasabi, Y.; Burgardt, P.; Lee, J.; Miryala, A.; Kusumaatmaja, W.; Carman, M. R.; Shtein, M.; Kieffer, J.; Lahann, J.; Kotov, N. A. *Langmuir* **2007**, *23*, 7901–7906.
(5) (a) Watanabe, S.; Regen, S. L. *J. Am. Chem. Soc.* **1994**, *116*, 8855–8856. (b) He, J.-A.; Valluzzi, R.; Yang, K.; Dolukhanyan, T.; Sung, C.; Kumar, J.; Tripathy, S. K.; Samuelson, L.; Balogh, L.; Tomalia, D. A. *Chem. Mater.* **1999**, *11*, 3268–3274. (c) Huo, F. W.; Xu, H. P.; Zhang, L.; Fu, Y.; Wang, Z. Q.; Zhang, X. *Chem. Commun.* **2003**, 874–875.
(6) (a) Zhang, X.; Gao, M. L.; Kong, X. X.; Sun, Y. P.; Shen, J. C. *Chem.Commun.* **1994**, 1055–1056. (b) Ariga, K.; Lvov, Y.; Kunitake, T. *J. Am. Chem. Soc.* **1997**, *119*, 2224–2231. (c) Advincula, R. C.; Fells, E.; Park, M. K. *Chem. Mater.* **2001**, *13*, 2870–2878.
(7) (a) Emoto, K.; Iijima, M.; Nakasaki, Y.; Kataoka, K. *J. Am. Chem. Soc.* **2000**, *122*, 2653–2654. (b) Ma, N.; Zhang, H. Y.; Song, B.; Wang, Z. Q.; Zhang, X. *Chem. Mater.* **2005**, *17*, 5065–5069. (c) Cho, J. H.; Hong, J. K.; Char, K.; Caruso, F. *J. Am. Chem. Soc.* **2006**, *128*, 9935–9942. (d) Qi, B.; Tong, X.; Zhao, Y. *Macromolecules* **2006**, *39*, 5714–5719. (e) Liu, X. K.; Zhou, L.; Geng, W.; Sun, J. Q. *Langmuir* **2008**, *24*, 12986–12989.
(8) (a) Kong, W.; Zhang, X.; Gao, M. L.; Zhou, H.; Li, W.; Shen, J. C. *Macromol. Rapid Commun.* **1994**, *15*, 405–409. (b) Lvov, Y.; Ariga, K.; Ichinose, I.; Kunitake, T. *J. Am. Chem. Soc.* **1995**, *117*, 6117–6123. (c) Picart, C.; Lavalle, Ph.; Hubert, P.; Cuisinier, F. J. G.; Decher, G.; Schaaf, P.; Voegel, J.-C. *Langmuir* **2001**, *17*, 7414–7424. (d) Serizawa, T.; Yamaguchi, M.; Akashi, M. *Macromolecules* **2002**, *35*, 8656–8658. (e) Yoo, P. J.; Nam, K. T.; Qi, J.; Lee, S. K.; Park, J.; Belcher, A. M.; Hammond, P. T. *Nat. Mater.* **2006**, *5*, 234–240.
(9) (a) Hiller, J. A.; Mendelsohn, J. D.; Rubner, M. F. *Nat. Mater.* **2002**, *1*, 59–63. (b) Zhang, L. B.; Li, Y.; Sun, J. Q.; Shen, J. C. *Langmuir* **2008**, *24*, 10851–10857.
(10) (a) Zhang, X.; Shi, F.; Yu, X.; Liu, H.; Fu, Y.; Wang, Z. Q.; Jiang, L.; Li, X. Y. *J. Am. Chem. Soc.* **2004**, *126*, 3064–3065. (b) Zhai, L.; Cebeci, F. C.; Cohen, R. E.; Rubner, M. F. *Nano Lett.* **2004**, *4*, 1349–1353. (c) Jisr, R. M.; Rmaile, H. H.; Schlenoff, J. B. *Angew. Chem., Int. Ed.* **2005**, *44*, 782–785. (d) Zhang, L. B.; Chen, H.; Sun, J. Q.; Shen, J. C. *Chem. Mater.* **2007**, *19*, 948–953.
(11) (a) Kang, E. H.; Jin, P. C.; Yang, Y. Q.; Sun, J. Q.; Shen, J. C. *Chem. Commun.* **2006**, 4332–4334. (b) Van Cott, K. E.; Guzy, M.; Neyman, P.; Brands, C.; Heflin, J. R.; Gibson, H. W.; Davis, R. M. *Angew. Chem., Int. Ed.* **2002**, *41*, 3236–3238. (c) Fischer, P.; Koetse, M.; Laschewsky, A.; Wischerhoff, E.; Jullien, L.; Persoons, A.; Verbiest, T. *Macromolecules* **2000**, *33*, 9471–9473.
(12) (a) Lvov, Y.; Caruso, F. *Anal. Chem.* **2001**, *73*, 4212–4217. (b) Calvo, E. J.; Danilowicz, C.; Wolosiuk, A. *J. Am. Chem. Soc.* **2002**, *124*, 2452–2453.
(13) (a) Mendelsohn, J. D.; Yang, S. Y.; Hiller, J.; Hochbaum, A. I.; Rubner, M. F. *Biomacromolecules* **2003**, *4*, 96–106. (b) Schneider, A.; Francius, G.; Obeid, R.; Schwinté, P.; Hemmerlé, J.; Frisch, B.; Schaaf, P.; Voegel, J.-C.; Senger, B.; Picart, C. *Langmuir* **2006**, *22*, 1193–1200. (c) Sinani, V. A.; Koktysh, D. S.; Yun, B.-G.; Matts, R. L.; Pappas, T. C.; Motamedi, M.; Thomas, S. N.; Kotov, N. A. *Nano. Lett.* **2003**, *3*, 1177–1182. (d) Lu, Y. X.; Sun, J. Q.; Shen, J. C. *Langmuir* **2008**, *24*, 8050–8055.
(14) (a) Chung, A. J.; Rubner, M. F. *Langmuir* **2002**, *18*, 1176–1183. (b) Ren, K. F.; Ji, J.; Shen, J. C. *Bioconjugate Chem.* **2006**, *17*, 77–83. (c) Serpe, M. J.; Yarmey, K. A.; Nolan, C. M.; Lyon, L. A. *Biomacromolecules* **2005**, *6*, 408–413. (d) Serizawa, T.; Matsukuma, D.; Nanameki, K.; Uemura, M.; Kurusu, F.; Akashi, M. *Macromolecules* **2004**, *37*, 6531–6536.
(15) (a) Jiang, S. P.; Liu, Z. C.; Tian, Z. Q. *Adv. Mater.* **2006**, *18*, 1068–1072. (b) Farhat, T. R.; Hammond, P. T. *Adv. Funct. Mater.* **2005**, *15*, 945–954.
(16) (a) Guldi, D. M.; Zilbermann, I.; Anderson, G.; Kotov, N. A.; Tagmatarchise, N.; Prato, M. *J. Mater. Chem.* **2005**, *15*, 114–118. (b) Guldi, D. M.; Rahman, G. M. A.; Prato, M.; Jux, N.; Qin, S.; Ford, W. *Angew. Chem., Int. Ed.* **2005**, *44*, 2015–2018.
(17) (a) Leväsalmi, J.-M.; McCarthy, T. J. *Macromolecules* **1997**, *30*, 1752–1757. (b) Bruening, M. L.; Sullivan, D. M. *Chem.—Eur. J.* **2002**, *8*, 3833–3837. (c) Park, M.-K.; Deng, S.; Advincula, R. C. *J. Am. Chem. Soc.* **2004**, *126*, 13723–13731. (d) Ball, V.; Voegel, J.-C.; Schaaf, P. *Langmuir* **2005**, *21*, 4129–4137. (e) Fujikawa, S.; Muto, E.; Kunitake, T. *Langmuir* **2009**, *25*, 11563–11568.
(18) (a) Yoo, D.; Shiratori, S. S.; Rubner, M. F. *Macromolecules* **1998**, *31*, 4309–4318. (b) Shiratori, S. S.; Rubner, M. F. *Macromolecules* **2000**, *33*, 4213–4219. (c) Mendelsohn, J. D.; Barrett, C. J.; Chan, V. V.; Pal, A. J.; Mayes, A. M.; Rubner, M. F. *Langmuir* **2000**, *16*, 5017–5023. (d) Joly, S.; Kane, R.; Radzilowski, L.; Wang, T.; Wu, A.; Cohen, R. E.; Thomas, E. L.; Rubner, M. F. *Langmuir* **2000**, *16*, 1354–1359.
(19) (a) Thünemann, A. F.; Müller, M.; Dautzenberg, H.; Joanny, J.-F.; Löwen, H. *Adv. Polym. Sci.* **2004**, *166*, 113–171. (b) Kabanov, V. In *Multilayer Thin Films: Sequential Assembly of Nanocomposite Material*; Decher, G., Schlenoff, J. B., Eds.; Wiley-VCH: Weinheim, Germany, 2003; pp 47−86. (c) Philipp, B.; Dautzenberg, H.; Linow, K.-J.; Kötz, J.; Dawydoff, W. *Prog. Polym. Sci.* **1989**, *14*, 91–172.
(20) (a) Thünemann, A. F.; General, S. *J. Controlled Release* **2001**, *75*, 237–247. (b) Buchhammer, H.-M.; Petzold, G.; Lunkwitz, K. *Colloid Polym. Sci.* **2000**, *278*, 841–847. (c) Petzold, G.; Buchhammer, H. -M.; Lunkwitz, K. *Colloids Surf., A* **1996**, *119*, 87–92.
(21) (a) Schuetz, P.; Caruso, F. *Colloids Surf., A* **2002**, *207*, 33–40. (b) Reihs, T.; Müller, M.; Lunkwitz, K. *Colloids Surf., A* **2003**, *212*, 79–95.
(22) Guo, Y. M.; Geng, W.; Sun, J. Q. *Langmuir* **2009**, *25*, 1004–1010.

(23) (a) Liu, X. K.; Dai, B. Y.; Zhou, L.; Sun, J. Q. *J. Mater. Chem.* **2009**, *19*, 497–504. (b) Zhang, L.; Sun, J. Q. *Chem. Commun.* **2009**, 3901–3903.
(24) (a) Müller, M.; Kessler, B.; Richter, S. *Langmuir* **2005**, *21*, 7044–7051. (b) Ouyang, W.; Müller, M. *Macromol. Biosci.* **2006**, *6*, 929–941.
(25) Cao, W. X.; Ye, S. J.; Cao, S. G.; Zhao, C. *Macromol. Rapid Commun.* **1997**, *18*, 983–989.
(26) Sun, J. Q.; Wu, T.; Liu, F.; Wang, Z. Q.; Zhang, X.; Shen, J. C. *Langmuir* **2000**, *16*, 4620–4624.
(27) (a) Feng, X. J.; Jiang, L. *Adv. Mater.* **2006**, *18*, 3063–3078. (b) Zhang, X.; Shi, F.; Niu, J.; Jiang, Y. G.; Wang, Z. Q. *J. Mater. Chem.* **2008**, *18*, 621–633. (c) Xia, D.; Brueck, S. R. J. *Nano Lett.* **2008**, *8*, 2819–2824. (d) Xie, Q. D.; Xu, J.; Feng, L.; Jiang, L.; Tang, W. H.; Luo, X. D.; Han, C. C. *Adv. Mater.* **2004**, *16*, 302–305.
(28) (a) Gu, Z.-Z.; Uetsuka, H.; Takahashi, K.; Nakajima, R.; Onishi, H.; Fujishima, A.; Sato, O. *Angew. Chem., Int. Ed.* **2003**, *42*, 894–897. (b) Schulte, A. J.; Koch, K.; Spaeth, M.; Barthlott, W. *Acta Biomater.* **2009**, *5*, 1848–1854.
(29) (a) Li, D.-F.; Wang, H.-J.; Fu, J.-X.; Wang, W.; Jia, X.-S.; Wang, J.-Y. *J. Phys. Chem. B* **2008**, *112*, 16290–16299. (b) Sun, T. L.; Tan, H.; Han, D.; Fu, Q.; Jiang, L. *Small* **2005**, *1*, 959–963. (c) Fan, H. L.; Chen, P. P.; Qi, R. M.; Zhai, J.; Wang, J. X.; Chen, L.; Chen, L.; Sun, Q. M.; Song, Y. L.; Han, D.; Jiang, L. *Small* **2009**, *5*, 2144–2148.
(30) (a) Hong, X.; Gao, X. F.; Jiang, L. *J. Am. Chem. Soc.* **2007**, *129*, 1478–1479. (b) Jin, M. H.; Feng, X. J.; Feng, L.; Sun, T. L.; Zhai, J.; Li, T. J.; Jiang, L. *Adv. Mater.* **2005**, *17*, 1977–1981. (c) Ishii, D.; Yabu, H.; Shimomura, M. *Chem. Mater.* **2009**, *21*, 1799–1801. (d) Winkleman, A.; Gotesman, G.; Yoffe, A.; Naaman, R. *Nano Lett.* **2008**, *8*, 1241–1245.